Pacific Northwest
NATIONAL LABORATORY

PNNL-35607

Chlorine Isotope Separations using Thermal Diffusion

M2AT-23PN1101046

January 2024

Zachary Huber
Michael Powell
Tyler Schlieder
Juan Cervantes
Jim Davis
Parker Okabe
Riane Stene
Tatiana Levitskaia
Bruce McNamara

U.S. DEPARTMENT OF ENERGY

Prepared for the U.S. Department of Energy
under Contract DE-AC05-76RL01830

DISCLAIMER

PACIFIC NORTHWEST NATIONAL LABORATORY
operated by
BATTELLE
for the
UNITED STATES DEPARTMENT OF ENERGY
under Contract DE-AC05-76RL01830

Printed in the United States of America

Available to DOE and DOE contractors from
the Office of Scientific and Technical Information,
P.O. Box 62, Oak Ridge, TN 37831-0062
www.osti.gov
ph: (865) 576-8401
fox: (865) 576-5728
email: reports@osti.gov

Available to the public from the National Technical Information Service
5301 Shawnee Rd., Alexandria, VA 22312
ph: (800) 553-NTIS (6847)
or (703) 605-6000
email: info@ntis.gov
Online ordering: http://www.ntis.gov

PNNL-35607

0BChlorine Isotope Separations using Thermal Diffusion

M2AT-23PN1101046

January 2024

Zachary Huber
Michael Powell
Tyler Schlieder
Juan Cervantes
Jim Davis
Parker Okabe
Riane Stene
Tatiana Levitskaia
Bruce McNamara

Prepared for
the U.S. Department of Energy
under Contract DE-AC05-76RL01830

Pacific Northwest National Laboratory
Richland, Washington 99354

Abstract

Molten chloride salt reactors need to use chlorine that is enriched in the isotope ^{37}Cl so the higher natural abundance ^{35}Cl does not interfere with neutronics and reactor operations. To this end, a thermal diffusion isotope separations (TDIS) apparatus was constructed in 2023. Successful shakedown testing was achieved and enrichments of isotopic concentrations relative to natural abundance $^{35/37}Cl$ were collected. Further, a multi physics model was validated and drove the timing for sampling and other critical extrapolated functions that are discussed herein. Necessary data needed for TDIS systems, such as the thermal diffusion coefficient, was measured with high precision for mission relative temperature ranges not previously reported in literature. These critical data points coupled with the validated model drove accurate estimates for column lengths needed to achieve desired enrichments for varying system temperatures are presented. Potential materials of construction are also discussed.

Our decision to move forward in 2024 with the installation of a larger set of separation tubes and associated equipment was based on the successful development of the predictive model and demonstration of small scale Cl enrichments. The Chlorine Isotopes Project Team at PNNL is prepared to claim that the installation and hence its separative power is restricted only by the spatial limitations of the laboratory, and this at present appears to be the limiting feature to first pass high enriched ^{37}Cl.

Acronyms and Abbreviations

DAC	data acquisition and control system
EMIS	electromagnetic isotope separation
HCl	hydrogen chloride, gaseous
MPP	multi physics package
MSR	molten salt reactor
MSFR	molten salt fast reactor
MSRE	molten salt reactor experiment
ORC	octupole collision/reaction cell
P&ID	process and instrumentation diagram
PNNL	Pacific Northwest National Laboratory
QQQ-ICP-MS	triple-quadrupole inductively coupled plasma mass spectrometry
RGA	residual gas analyzer
TDIS	thermal diffusion isotopic separation

Contents

Figures

Tables

1.0 Introduction

The use of chloride salts in Molten Salt Reactors (MSR) provide some benefits over the use of fluoride salts. Chloride salts have higher actinide solubility therefore can accommodate higher fuel loadings allowing for larger fission product buildup within a reactor. Additionally, chloride-based reactors operate at fast neutron spectrums, so they can improve breeding and burning in reactor. Despite their operational benefits, chloride salts are also plagued by some downsides when compared to fluoride salts. A chloride reactor has more complex corrosion issues that have significant material of construction challenges. Chlorine also has two isotopes, of which ^{35}Cl has a significant neutron capture cross section and higher natural abundance than ^{37}Cl (^{35}Cl ~76% and ^{37}Cl ~24% natural abundance).

The significant neutron capture cross section of ^{35}Cl (~42 barns) poses multiple problems. First, when capturing a neutron, it can transmute to ^{36}Cl which is radioactive. Due to the high environmental mobility and solubility of Cl, the long-lived half-life of 301,000 years, and the strong beta emission during ^{36}Cl decay (709 keV), this is an undesirable byproduct of chloride salts under irradiating conditions. Secondly, the neutron capture results in sulfur production which forms extremely corrosive compounds thus making the chloride salt corrosion issues more complex. Lastly, the large capture cross section reduces the neutron economy of the reactor as it acts like a poison.

The present work investigates the enrichment of ^{37}Cl, thereby reducing the abundance of ^{35}Cl for use in chloride based MSR. While multiple methods exist or are proposed for the enrichment of Cl isotopes to solve issues related to ^{35}Cl, this work proposes an existing and proven technology to enrich the lesser abundant ^{37}Cl: thermal diffusion isotope separation (TDIS). The use of hydrogen chloride (HCl) is chosen as it provides a readily useable reagent for generation of chloride salts. Some data also exists for Cl isotope separations in this matrix which provided a convenient starting location for the implementation of this method. The mathematical treatment of TDIS is well documented and coincides well with existing work at PNNL using similar and complementary systems for other separations. Alternate enrichment methodologies are discussed briefly in later sections.

The existence of thermal diffusion was first predicted by Enskog in 1911 in his doctoral thesis and was first demonstrated by Chapman and Dootson in 1917. Clusius and Dickel (1939) achieved a critical success in the separation of HCl into its isotopic components. Kennedy and Seaborg (1940) used a similar approach to separate $H^{37}Cl$ from $H^{38}Cl$ and $^{1}H_2$ from $^{3}H_2$.

The underlying working concept of thermal diffusion is that a sufficiently tall separation tube provides for high enrichments of elements and their isotopes. In the referenced cases, the separation devices were made from Pyrex glass and their heights exceeded 7 meters. Experiments showed that the same efficacy of separation could be had by a series arrangement of shorter tubes [Schrader 1946]. First pass separations of $^{35/37}Cl$ were reported to exceed 99% ^{37}Cl enrichment in such devices.

The investigation at PNNL was initiated with literature searches concerning isotope separations that began in early 1900's. During a decade of concern whether or not the existence of non-radioactive isotopes were the imaginations of experimental scientists [Thompson 1913], pivotal gravimetric experiments that promoted tiny enrichments of the chlorine isotopes of gaseous, anhydrous, hydrochloric acid $^{35/37}Cl$-H were achieved [Harkins 1922]. The descriptors for HCl remind us that in those times HCl was not a commercial product, and it's pure and anhydrous

preparation on a multi-liter scale was only the first crucial step in probative studies of its enrichment.

2.0 Methods of Isotope Separations

In his experimental study on the molecular mobility of gases in 1893, Graham distinguishes for us the principles of (1), effusion through small apertures, in which there is practically no friction, different gases develop a mass motion whose velocity is inversely proportional to the square root of their molecular weight; (2), capillary transpiration, in which the rate of mass motion is greatly reduced by friction; and (3), molecular diffusion, for which the rates of molecular diffusion of different gases also vary inversely as the square roots of their molecular weights. These or combinations of them, formed the basis for the known gaseous isotope separations: gaseous diffusion, centrifugation, thermal diffusion. Distillation, chemical exchange reactions, and electrolytic methods depend on intermolecular forces and have been useful for hydrogen isotope separations [Vogel 2022, Rae 1978], whereas the use of electromagnetic fields (calutron) has been successfully demonstrated for high purity separation and collection of the isotopes of a diverse set of elements [Smith 2013, Abramychev 1992].

Several aspects of the application of the chlorine isotope separation narrows down significantly the available methodologies to electromagnetic separative techniques, centrifuge, and thermal diffusion. Firstly, the time horizon required for general use of enriched ^{37}Cl by way of its use in chloride form MSFRs might be 5 -10 years, and its use for experimental study is at hand. Second, the use of HCl as a precursor synthetic reagent likely cannot be overstated. Initial thoughts include production of alkali, alkaline earth chlorides, actinide chlorides for fertile materials, and reagents, e.g., $NH_4{}^{37}Cl$ and $C^{37}Cl_4$ that researchers today are considering in the laboratory for synthetic production of the actinide chlorides. It remains to be seen if $H^{37}Cl$ or $NH_4{}^{37}Cl$ solid/ gas will be used as the desiccant /reductant combination (HF/H_2) commonly used in final batch production for the MSRE [Lindauer 1967].

It would appear that the quantity of $H^{37}Cl$ required in a timely fashion would eliminate electromagnetic isotope separation (EMIS) providers assuming ionization didn't negatively impact the separation. Chlorine isotope separations using HCl, in particular by centrifuge, should be pursued and could become a viable market in the future. The mathematics of isotopic separations by thermal diffusion and centrifuge intersect in the early 1900's and then again intersect and disentangle in the 1940's. As the centrifuge operation deviates from its initial designs as built around the $^{235/238}U$ separation, to those of lower mass below 80 amu [Borisevich 2000, Kaliteevskny 2023], the efficacy of the design will depend in part on building a predictive model that accounts for the interaction of the working gas and the apparatus. It will be seen in this work that the design of an efficient multi-stage operation is similar in concept to those used in centrifuge operations and can be used effectively given a working numerical model.

The reasons for the preferred use of HCl are indicated above. The use of Cl_2 is also reasonable for the same reasons, however the centrifuge operation does not provide an ionizing mechanism. Molecules such Cl_2 and CCl_4, additionally are a statistical mixture of the Cl isotopes, and ones such as CH_3CH_2-Cl do not provide an easy access Cl for the chemical requirements of the molten salt community. In a centrifuge cascade, the low chlorine isotopic masses will require an updated rotor design [Kaliteevskny 2023] and will likely impose low mass related transport issues for the cascading operation. Further, HCl may cause intolerable corrosion rates of delicate internal surfaces [Borisevich 2000]. It appeared to the PNNL team that the level of research into this endeavor was outside the funding, as well as the time horizon for its successful implementation.

2.1 An Optimized Model for the TDIS in HCl

Although chlorine isotope separations to high enrichment in ^{37}Cl have been achieved using thermal diffusion [Clusius 1939, Shrader 1946, Kennedy 1940], the separations were never extended to large scale, as there were no industrial uses for the material. The method was chosen by the PNNL team for the reasons cited above and further because of the available, well-developed mathematical treatment of thermal diffusion of isotopic gas systems. The mathematical basis was important to the construction and application/validation of a predictive model, not only for design of the separative apparatus, but additionally for validating experimental data and permitting predictive aspects of operation such as:

- time to equilibrium (start-up period for data collection)
- data collection times - how long to reach equilibrium temperature/pressure set points
- single stage enrichment prediction/validation from tube length and temperature of separation
- measurement of the thermal diffusion constant, α (see model)
- enrichment calculation for multiple serially arranged columns
- production rate for constant flowing gas into the system and extracting gas from the heavy end of the column (hereafter referred to as bleed and feed)
    1. number of stages required for bleed and feed operation
    2. optimized feed rates
    3. optimized recycle of tail fractions to feed
    4. power requirements

2.2 An Optimized Apparatus for the Thermal Diffusion of HCl

The design of a generalized separations apparatus was based on a transport model provided by Green 1966. Majority of the information in the following equations is calculated from known physical data of HCl, such as its temperature dependent density, and the geometry of the separation apparatus. The transport equation is given by Equation 1 below.

$$\tau = Hx(1-x) - (K_c + K_d)\frac{dx}{dz} \tag{1}$$

where τ is the net transport of light component toward the top of the column, x is the mole fraction of the light component in the mixture, z is the axial column coordinate, and H, K_c, and K_d are the transport coefficients defined further in Equation 2:

$$H = \frac{2\,\pi\,\alpha\rho^2 g}{6!\;\mu}\cdot r_{avg}\,(r_1 - r_2)^3\left(\frac{T_{hot} - T_{cold}}{T_a}\right)^2 \cdot h_m \tag{2}$$

$$K_c = \frac{2\,\pi\,\rho^3 g^2}{9!\;\mu^2 D}\cdot r_{avg}\,(r_1 - r_2)^7 - \left(\frac{T_{hot} - T_{cold}}{T_a}\right)^2 \cdot k_c$$

$$K_d = 2\,\pi\rho D\;\cdot\; r_{avg}\,(r_1 - r_2)\cdot\; k_d$$

Here α is the thermal diffusion constant of HCl. Once the geometry of the separation column shown in Figure 1 is known, α is the only unknown, D is the ordinary coefficient of diffusion of HCl, g is the gravitational constant, ρ is the density of HCl, and μ is the the viscosity of HCl. All constants are taken at the average temperature (T_a). T_{cold} and T_{hot} are the measured cold and hot wall temperatures, respectively. See Figure 1 for locational definitions of r1 and r2, and T_{cold} and T_{hot}.

One can see that to calculate the transport coefficient, τ, the known physical constants for HCl are required. The constants h_m, k_c, and k_d are discussed below. Consequently, with estimates of the actual values of the geometric features of the apparatus as a starting point, one can calculate α from the transport coefficients.

Specifically, the separations column is a tube in a tube. The outer tube is jacketed and cooled to near room temperature with water. The inner tube is internally heated with cartridge heaters.

The gap between the hot wall (T_{hot}) and the cold wall (T_{cold}) is filled with HCl gas. The lighter component $H^{35}Cl$ moves up the column faster than the $H^{37}Cl$ component, which itself is attracted to the cold wall, is cooled, and slows down.

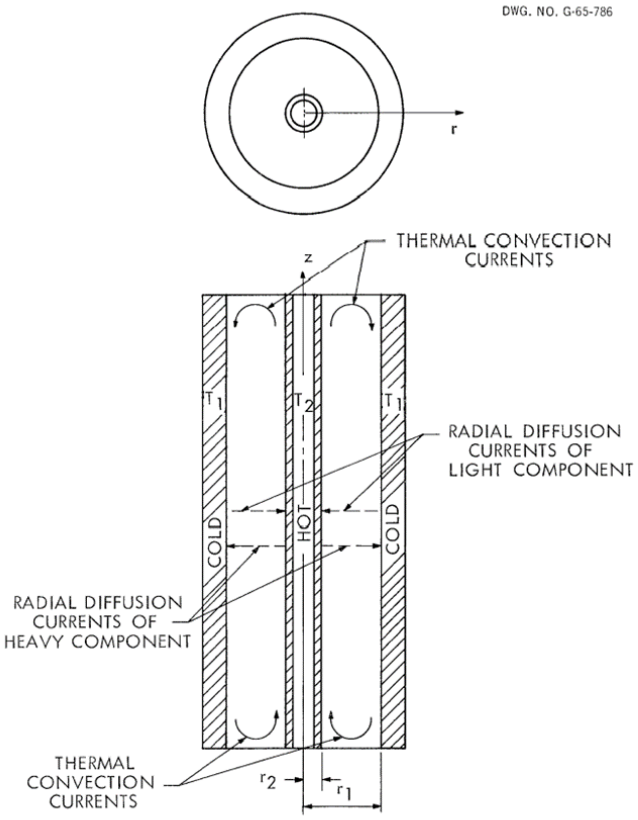

Figure 1: The separation column for TDIS is a tube inside of a tube where thermal convection currents and radial diffusion work to provide the isotope separation.

The α value is sensitive to the type of interaction between the molecules forming the gas. All the molecules in the gas repel one another with a force which varies as the inverse v^{th} power of the distance of separation and the molar heat capacity of the gas is independent of temperature.

For systems polar molecules like HCl, the thermal diffusion constant, α, is positive for $v>5$, whereas it is negative for $v<5$. The fact that the value of α depends so critically on the nature of the intermolecular forces means that free-path arguments of elementary kinetic theory are quite inadequate for the treatment of thermal diffusion. Over time the kinetic theory of gases evolved and the paper by Green et al (1966) conveniently provides the "shape factors" h_m, k_c and k_d as constants for a large set of small molecules across a relevant temperature range so they may be looked up and inserted into the calculation of the transport coefficients, H, K_d, K_c.

Accordingly, values of the coefficient of thermal diffusion, α, were initially searched out in the literature [Kranz 1953, Shrader 1946, Clusius 1939, Kennedy 1940, Akabori 1941] which are plotted in Figure. 2. The fit to the data implies: α = 9.64E-6*T – 2.67E-3.

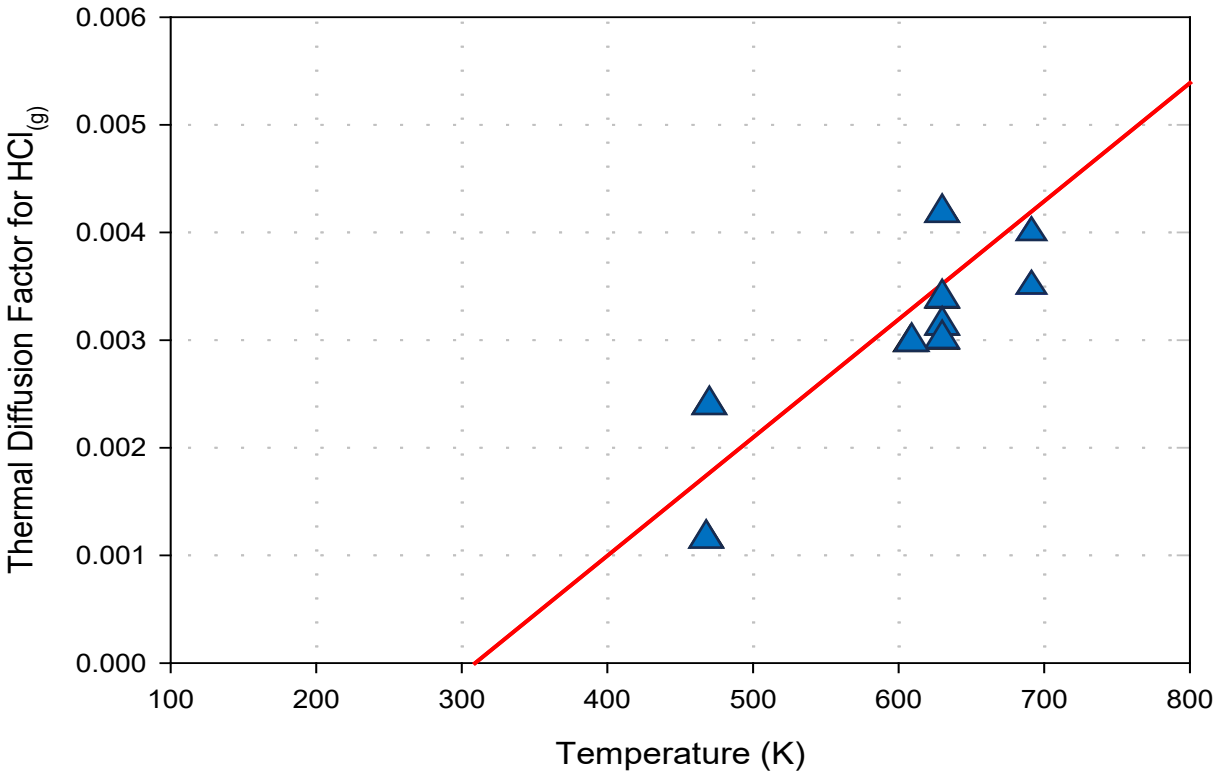

Figure 2 Literature values of coefficient of thermal diffusion, α for $HCl_{(g)}$. The red line is a best fit linear approximation.

The predicted temperature where α = 0 is about 310 K. Determining this zero-crossing point is important for setting the minimum value for T_{cold}. With these, assumptions were made concerning iterative values of T_{hot} and geometric parameters, R= r1 / r2, that is the gap distance between the tubes, and the column length, L. These fix the effects of the column dimensions on the separations and allow iterative calculation of the equilibrium separation factor q_e to be quantified, with change in dimensions, in α, or in T_{hot} and T_{cold}.

2.3 TDIS Column Design

The TDIS model and its use for design of the separations columns was described by McNamara 2023 and are reproduced here in part for purposes of continuity. Given the literature average value for α from Figure 2, one can calculate values for H, L, and K. Thus, per Equation 1, for the equilibrium separation concentrations of $H^{35}Cl$ and $H^{37}Cl$:

$$q_e = \exp\left(\frac{HL}{K}\right) = \frac{c_L(1-c_0)}{c_0(1-c_L)} \quad (3)$$

where c_L is the mole fraction of $H^{35}Cl$ at the "light" end of the separation column and c_0 is the mole fraction of $H^{35}Cl$ at the "heavy" end. For the case where $H^{37}Cl$ is being produced, c_L = ~0.75 when the light end of the column is connected to a large reservoir (or continuous flow in/out) natural abundance HCl. Once H and K are estimated based on the column design, the minimum total column length required for the desired separation can be calculated from the above equation. This length represents the minimum required length because the equation gives the equilibrium separation.

Our column sizing calculations analysis imply that a channel gap of about 4-5 mm will maximize isotopic separations of HCl where the analyses are based on available data for α and the target operating pressure is in the range of 1-2 atm (absolute). At higher operating pressures, the optimal channel gap is narrower, but the relatively small benefits of operating at higher pressure are negated by the difficulties associated with building columns with very narrow channel gaps. On the basis of these tradeoffs, we selected a target channel gap of 4-5 mm for our demonstration TDIS columns (Figure 3).

The design parameters included:

1. Use 2.5-inch Schedule 40 pipe for innermost tube
    a. ID = 6.27 cm; OD = 6.96 cm (after OD grinding)
2. Use 3.0-inch Schedule 40 pipe for cold wall between HCl and cooling water
    a. ID = 7.90 cm (after honing); OD = 8.89 cm

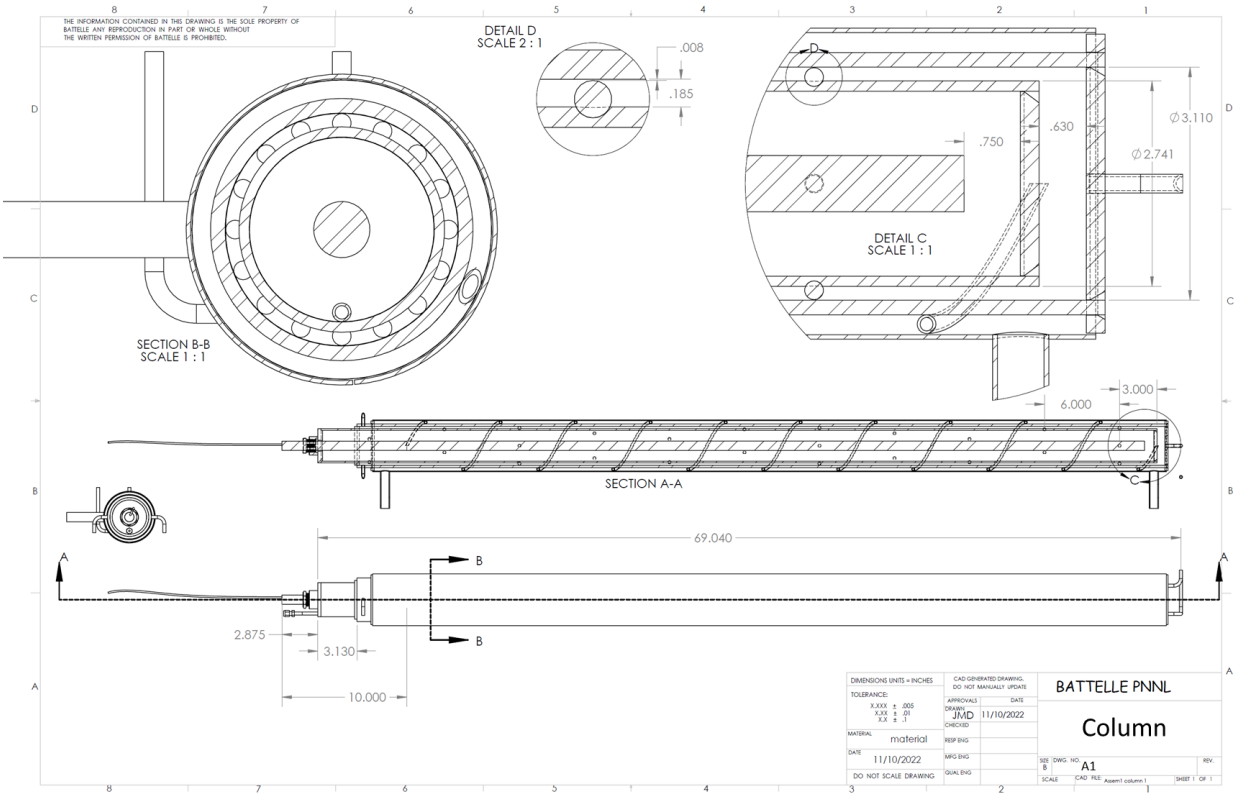

Figure 3: Engineering drawing of the column design. All dimensions are in inches.

For ease of construction and to use materials that were well known, easily obtainable and readily machinable, the use of an Inconel 600 inner tube was chosen to provide the T_{hot} surface and a stainless steel 316L outer tube forms the T_{cold} surface.

The outer cooling jacket (providing T_{cold}) was formed by wrapping a spiral of 6.35 mm stainless steel rod around the 8.89 cm pipe and then adding a sheet-metal outer jacket. Divots were machined into the innermost pipe and 6.35 mm polished stainless steel 316L ball bearings were placed in the divots during assembly. These will maintain the pipe centering with constant gap thickness and allow for axial movement due to thermal expansion. The bearings have since been changed to Inconel 600 to reduce the corrosion potential inside the columns.

The overall length of the completed assembly is approximately 183 cm. The cartridge heaters (providing T_{hot}) extend out about 15 cm farther from the top. Total effective length for thermal diffusion separation is about 162 cm per column (i.e., L = 162 cm). The resulting channel gap is approximately 4.5 mm (providing r_1-r_2) at operating temperature of T_{hot} = 300 - 400°C.

The piping and instrumentation diagram (P&ID) for the total apparatus is shown below in Figure 4. On the left hand side of the P&ID is the HCl fill equipment, in the center are the two separations columns and on the right hand side is the sampling apparatus, the vacuum pumps needed to remove and/or move gases through the system, and a helium backfill setup to increase heat transfer for the cartridge heaters inserted into the center tube of the columns.

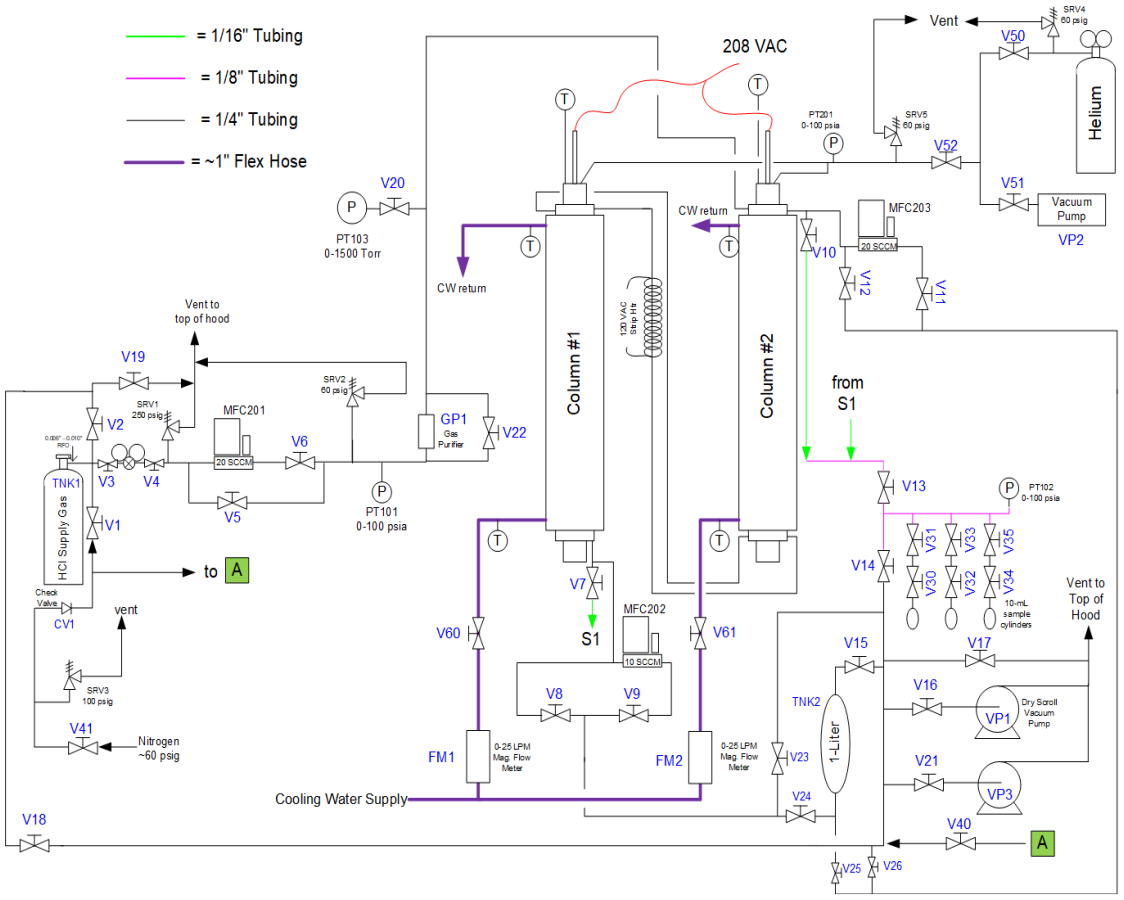

Figure 4: P&ID for the columns and associated apparatus. The left hand side provides the HCl gas feed to the system, the center is the separation columns, and the right hand side is the sampling, vacuum, and He backfill setup.

2.4 Current Operations of the TDIS system

The TDIS apparatus was built in the 1st quarter of 2023 and its shakedown testing was completed in July of 2023. Figure 5 shows the separation system's two, 6-foot separations columns on the right and the data acquisition and control system (DAC) as borrowed from the TDIS group at PNNL. The two serially connected column system is currently operational. It is located inside of a walk-in fumehood. In addition to the P&ID and the DAC, it features an HCl gas monitoring system for safety that will automatically shutdown and notify operators in the unlikely event of a controller malfunction or gas leak detection. Each individual column has an internal volume of approximately 1.7L giving a total internal gas volume of 3.4L available for HCl.

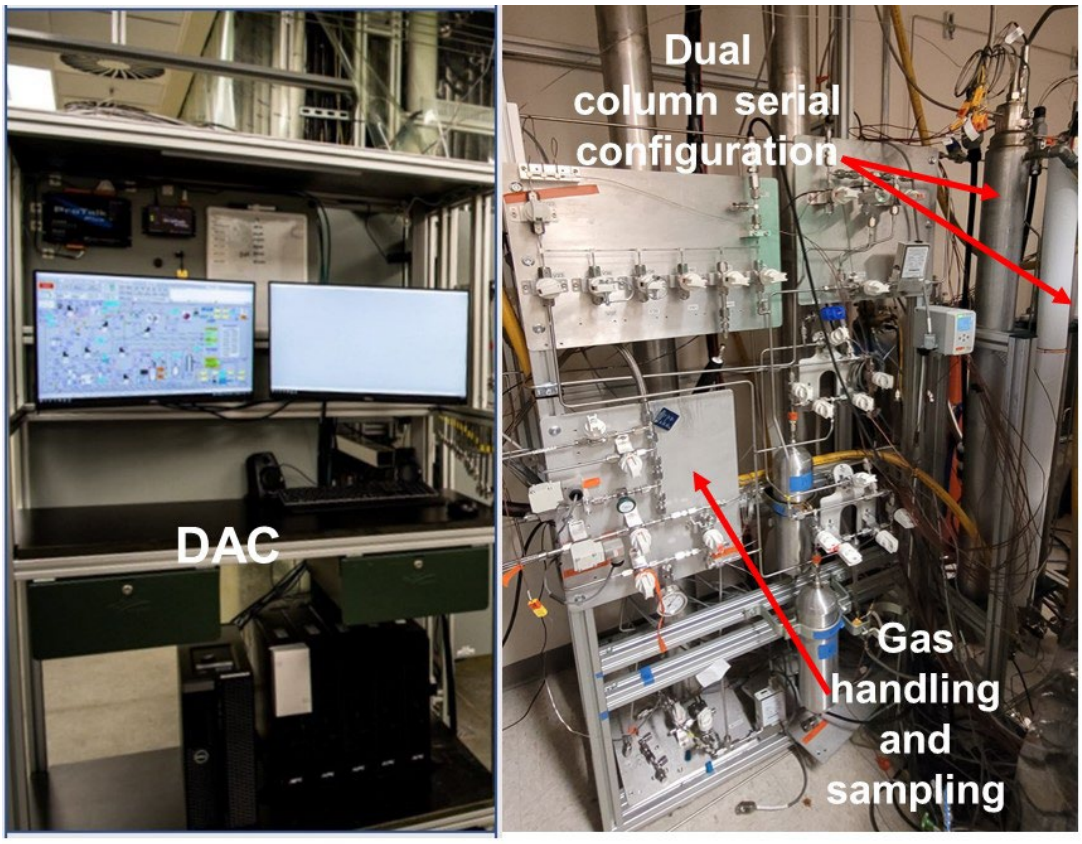

Figure 5: TDIS system as installed at PNNL. The left image shows the data acquisition and control system computer (DAC), and the right image shows the columns and gas handling. The DAC is located outside of the fumehood and the columns and gas handling is inside of a walk-in fumehood. The gas introduction system and the vacuum pumps are not shown in this picture but exist on the left side of the fumehood.

3.0 A New Method for Chlorine Isotopic Analysis

A method for measuring chlorine isotopic ratios using triple-quadrupole inductively coupled plasma mass spectrometry (QQQ-ICP-MS) as a means of validating ^{37}Cl enrichment was developed. The methodology, precision, and accuracy were discussed in a previous report (McNamara 2023) and is reproduced in Appendix C. All measurements made to date have used this new method.

The method requires a dilute aqueous solution to be introduced into the QQQ-ICP-MS. To do this, the gaseous HCl must be converted to a liquid. Starting at the TDIS system, the gas bulb is first heated and evacuated. It is then filled with HCl at the TDIS systems operating pressure and then pressurized to approximately 350 kPa with Ar. The gas bulb is then connected to a simple constructed system (See Figure 6) that consists of a 0.25 mm internal diameter by 1.5 m long capillary tube connected to the gas sample bulb through a VCR fitting. The open end of the capillary is positioned below the liquid surface of a clean scintillation vial filled with 5 mL deionized water. The gas is then bubbled through the water for approximately 10 minutes. The Ar pressurization is used as a carrier gas to push the HCl gas through the capillary and into the water. This creates a hydrochloric acid solution as the gas reacts with the water. After the sample is exhausted, the capillary is then disconnected and hooked up to a flowing Ar purge line and heated for five minutes to remove residual gas that has stuck to the walls of the capillary. The heating and purging reduce the likelihood of cross-contamination between the samples run through the same capillary tube. The prevention of cross-contamination was confirmed through blanks and a series of tests using known isotopic ratios of feed gas alternated with enriched gas samples. The dilute hydrochloric acid liquid samples are then ready for introduction into the QQQ-ICP-MS for analysis.

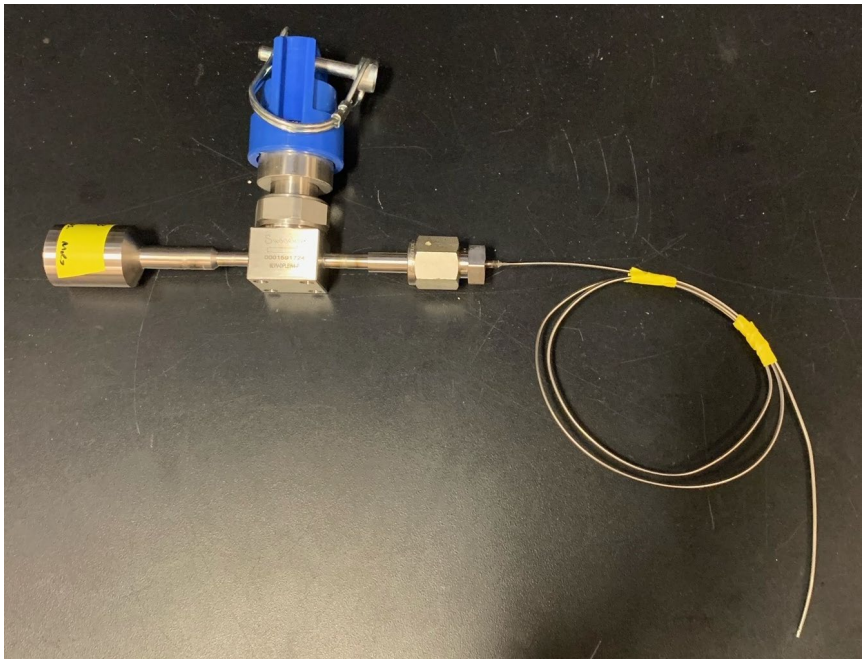

Figure 6: Image of the gas to aqueous conversion system.

Due to the laborious nature of conversion from gas to liquid for analysis, the use of a residual gas analyzer (RGA) is now being evaluated for online screening of the $^{35,37}Cl$ enrichment. In order to supplement the enrichment data in real-time, it has been determined that the RGA can

be used to give preliminary results of each experiment by analyzing the gas for $^{1}H^{35}Cl$ and $^{1}H^{37}Cl$. The RGA also utilizes a quadrupole mass filter at low pressures (10^{-7} to 10^{-4} Torr) to analyze a gas stream through a range of masses. A SRS RGA 100 (Stanford Research Systems, Sunnyvale, CA, USA) was used to measure masses from 1 to 100 amu. Furthermore, the RGA may also be useful in determining increased levels of corrosion to the system by analyzing for H_2, which would result from the reaction of HCl with metal. The only mass interferences of concern are Ar isotopes ^{36}Ar and ^{38}Ar, which have a natural abundance of 0.334% and 0.063%, respectively (Kondev 2021). These natural abundance values are low, and Ar should not be present in the system, thus are not of concern. The use of the RGA may be extended to the detection in-line of hydrogen gas to monitor corrosion rates in future work.

In order to validate this method, the tank of HCl gas used for the separation system was filled into a gas sample bulb and analyzed with He carrier gas to compare to the QQQ-ICP-MS results. Helium was used as the use of Ar would create the isobaric interferences discussed above. The RGA found a feed gas mass ratio $^{1}H^{37}Cl/^{1}H^{35}Cl$ of 0.3195 ± 0.0019 and the QQQ-ICP-MS found 0.3176 ± 0.0025, a 0.6% difference.

After the positive result of the first RGA test, eight more tests were conducted with natural and enriched isotopic ratios. The results of the nine tests can be seen in Table 1. The accuracy of the RGA is substantially lower than the QQQ-ICP-MS, but it still provides an excellent method for quick confirmation testing. While for the needs of this project, the QQQ-ICP-MS accuracy is needed for high fidelity measurement of the thermal diffusion coefficient, industrial operations may utilize an RGA as a constant system health monitoring tool. This brief, but important, investigation of the RGA proves the usefulness as a diagnostic type tool.

Table 1: Comparison of $^{37}Cl/^{35}Cl$ measured ratios for the RGA and QQQ-ICP-MS data.

	RGA		QQQ-ICP-MS		Difference (%)
Sample	**Mean**	**STD**	**Mean**	**STD**	
Feed Gas 1	0.3195	0.0019	0.3176	0.0025	0.6
Feed Gas 2	0.2742	0.0078	0.3176	0.0025	-13.7
Feed Gas 3	0.3400	0.0021	0.3176	0.0025	7.1
Enriched Gas 1	0.4111	0.0083	0.3934	0.0009	4.5
Enriched Gas 2	0.3822	0.0095	0.4143	0.0015	-7.7
Enriched Gas 3	0.4048	0.0079	0.4161	0.0023	-2.7
Enriched Gas 4	0.4368	0.0039	0.4173	0.0015	4.7
Enriched Gas 5	0.3905	0.0075	0.4124	0.0030	-5.3
Enriched Gas 6	0.4558	0.0189	0.4142	0.0024	10.1

4.0 Results and Discussion

4.1 Shakedown Testing of the TDIS System

Shakedown testing data for the new columns using Ar, specifically lower natural abundance ^{38}Ar (0.068%) and ^{36}Ar (0.334%), is shown in Figure 7. An in-line RGA was used to monitor the Ar isotopes in real time. Initial testing results were skewed to lower than the predicted behavior, especially at 400°C. Thermal gradient effects were verified as causative of the data malalignment using COMSOL Multiphysics Package (MPP) and new data was acquired using the improved temperature profiles.

COMSOL thermal modeling showed that most of the discrepancy between model-predicted and observed enrichment was due to non-uniform temperature profile effects. The measured hot side temperature distributions of our system are shown in Figure 8. The result gives us added confidence in the model predictions as well as our ability to back out alpha values for HCl based on TDIS column tests. This result also highlights the importance of quantifying the vertical temperature profile within the columns.

Figure 7 indicates that the enrichment of ^{36}Ar is asymptotic in time. The flattening out of the separation factor (Equation 1) is a function of the tube length if all other features of the tube geometry are optimized. The result demonstrated that the tubes were working for the ^{36,38}Ar separations between 200- 400°C hot wall temperatures.

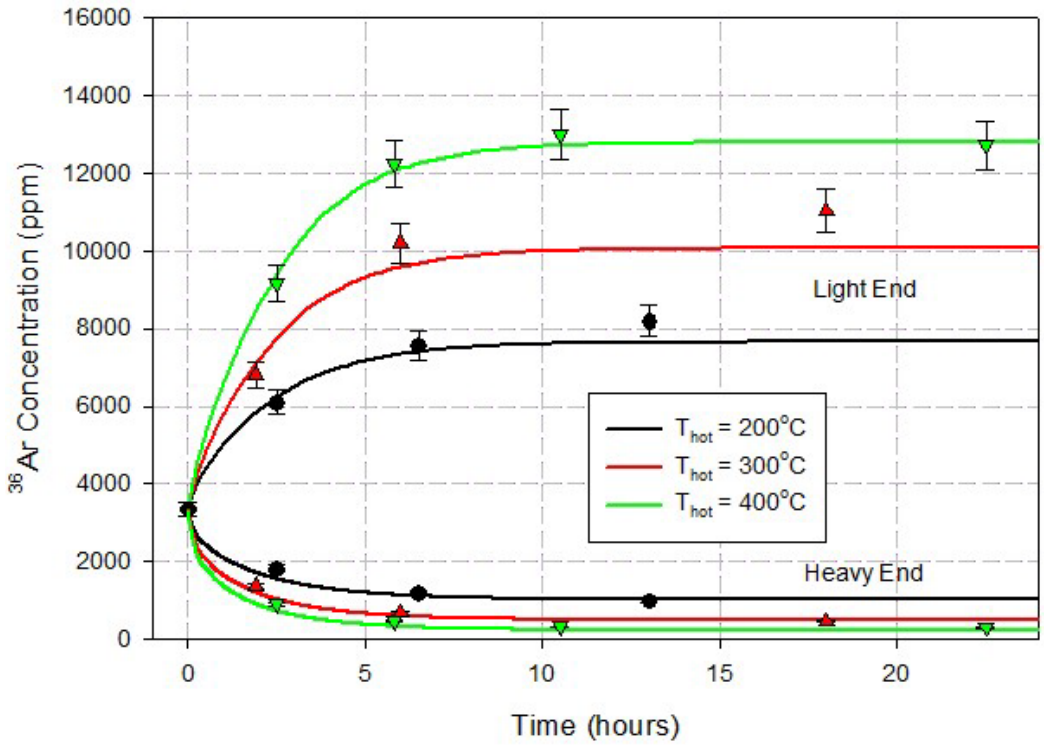

Figure 7: The measured isotopic enrichment of ^{36}Ar vs. time based on an assumed uniform hot-side temperature profile. The points are measured data from an RGA with error bars. The solid lines are predicted based on the COMSOL MPP model using known Ar constants for TDIS.

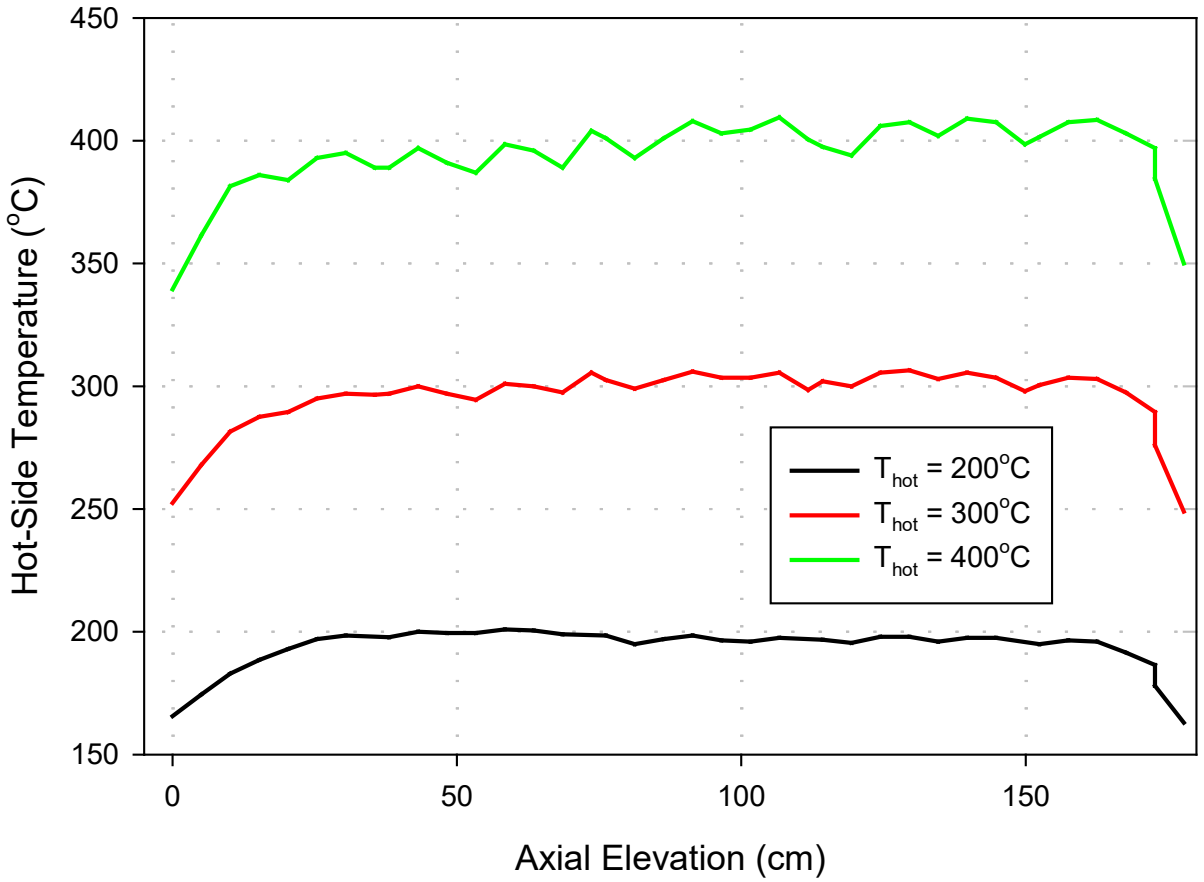

Figure 8: Measured temperature distributions within the TDIS columns. During measurement of the thermal diffusion coefficients of $HCl_{(g)}$ these temperature distributions were used as input to the COMSOL MPP model to increase accuracy.

The separation factor for a given column geometry is predicted by Equation 3. Figure 9 shows the predicted concentration of $H^{37}Cl$ at the bottom end (heavy side) of the column at 0.84 atm and T_{hot} = 400 ˚C. As a consequence of the prediction, and after the system has reached thermal equilibrium, the feed gas is introduced to the columns and data collected over the predicted time until the enrichment process is completed (15-20 h) for a given temperature. The increasing enrichment over time behavior shown in Ar and predicted for HCl is referred to as the startup dynamics behavior of a TDIS system. The length of startup time increases with increasing total length of the TDIS columns. Once the asymptote is reached, the system is considered to be in equilibrium. After startup dynamics of the TDIS system were determined, all subsequent sampling of gas for enrichment measurement happened well after the equilibrium enrichment was reached.

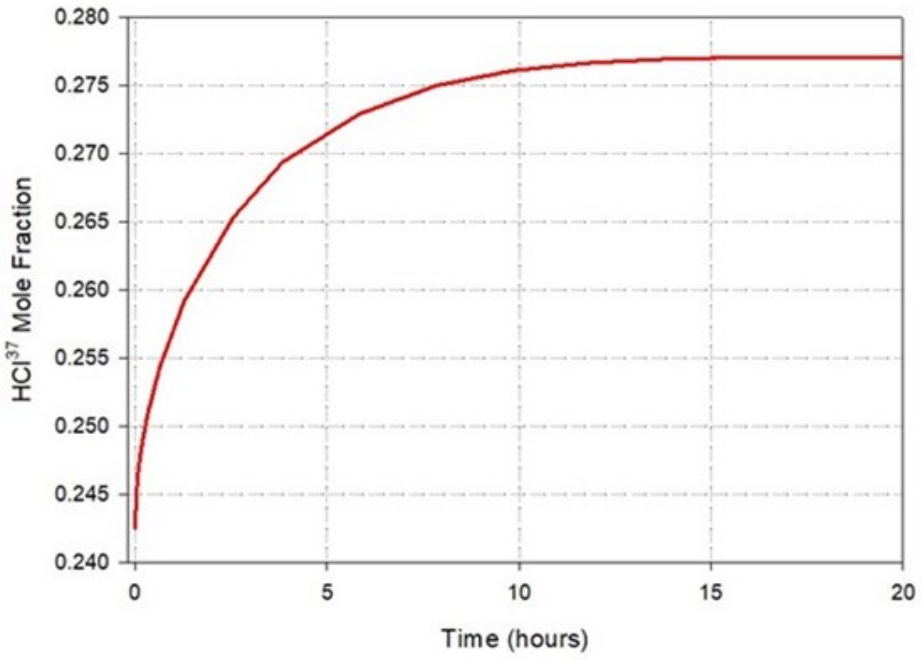

Figure 9: Predicted concentration of $H^{37}Cl$ at the heavy side (bottom) of the PNNL TDIS system using the model at 0.84 atm and T_{hot} = 400°C.

4.2 New Measurements of the Thermal Diffusion Constant, α for HCl

Measurement of the temperature and pressure dependences in the thermal diffusion constant α, was undertaken. Table 2 shows a summary of all tests conducted. Table 3 shows the flow rates used for Tests 11-15 where the system was run in the bleed and feed mode. All other tests were conducted at infinite reflux with no inlet or exit flows. The tests were specifically chosen to verify and bound the model predictions for pressure and temperature dependence of the thermal diffusion constant. The bleed and feed type tests are important for validating the model's use in predicting production environments where the operation would constantly separate and produce an enriched product gas. Unfortunately, during the 400 °C bleed and feed tests, there were pressure and flow stability issues related to the tuning on the flow controller. Additionally, the higher flow rate used in these tests (Test 14 and Test 15) potentially disrupted the convective flow near the light end of the column causing additional issues. These data points are not being used in the model correlation currently due to the high likelihood of inaccuracy. These tests will need to be redone with lower flow rates and after the flow controller tuning issues are addressed.

Figure 10 shows the temperature dependence juxtaposed with literature data as was plotted in Figure 2. It can be seen that the thermal diffusion coefficient, α, markedly increases with temperature. The higher temperature literature data was acquired from the incidental use of glass separations columns. The use of glass in natural physics experiments was common to premodern times. The magnitude of the diffusion constant increases the value of the transport coefficient, H in Equations 1 and 2. Consequently, the higher temperature (>600°C) data indicate that increased enrichments can be accessed using shorter or fewer columns.

High fidelity measurement of the temperature dependence in α tightens up the precision in the model for larger column design predictions. It appears that the lower temperature data collected from the TDIS system, as plotted in Figure 10, is more precise than the scattered data set assembled from the literature. It is likely this is due to the increased accuracy and precision measurement of enrichments enabled by the QQQ-ICP-MS method.

Table 2: Summary of all tests run in the PNNL TDIS system. Tests 1-10 and 16 are conducted at infinite reflux (i.e. no inlet or exit flows). Tests 11-15 are run as feed and bleed and therefore do not sample at the light end of the column.

Test #	T_{hot} (°C)	T_{cold} (°C)	T_{avg} (°C)	Pressure (atm)	^{37}Cl Fraction Light End	^{37}Cl Fraction Heavy End	Thermal Diffusion Factor
1	200	12	106	0.667	0.230	0.257	0.00127
2	200	12	106	0.595	0.229	0.257	0.00133
3	200	12	106	0.524	0.231	0.258	0.00138
4	290	12	151	0.976	0.221	0.269	0.00202
5	290	12	151	0.803	0.217	0.274	0.00205
6	290	12	151	0.697	0.216	0.276	0.00207
7	290	12	151	0.626	0.222	0.272	0.00181
8	330	12	171	0.963	0.214	0.276	0.00227
9	330	12	171	0.691	0.213	0.289	0.00235
10	330	12	171	0.597	0.214	0.284	0.00240
11	375	12	194	0.988	NA	0.294	0.00249
12	375	12	194	0.989	NA	0.292	0.00239
13	375	12	194	0.989	NA	0.293	0.00249
14	400	12	206	1.045	NA	0.293	0.00220
15	400	12	206	1.042	NA	0.294	0.00220
16	400	12	206	1.033	0.225	0.304	0.00225

Table 3: Flow rates for bleed and feed operation. All units are in standard cubic centimeters per minute (sccm). All flows are measured using flow controllers (with slightly varying accuracy) and the summation of heavy and light side flows equal the feed flow rate.

Test #	Feed Flow	Light Side Flow	Heavy Side Flow
11	10	9	0.94
12	10	9	0.94
13	10	9	1
14	15	14.4	0.625
15	15	14.4	0.625

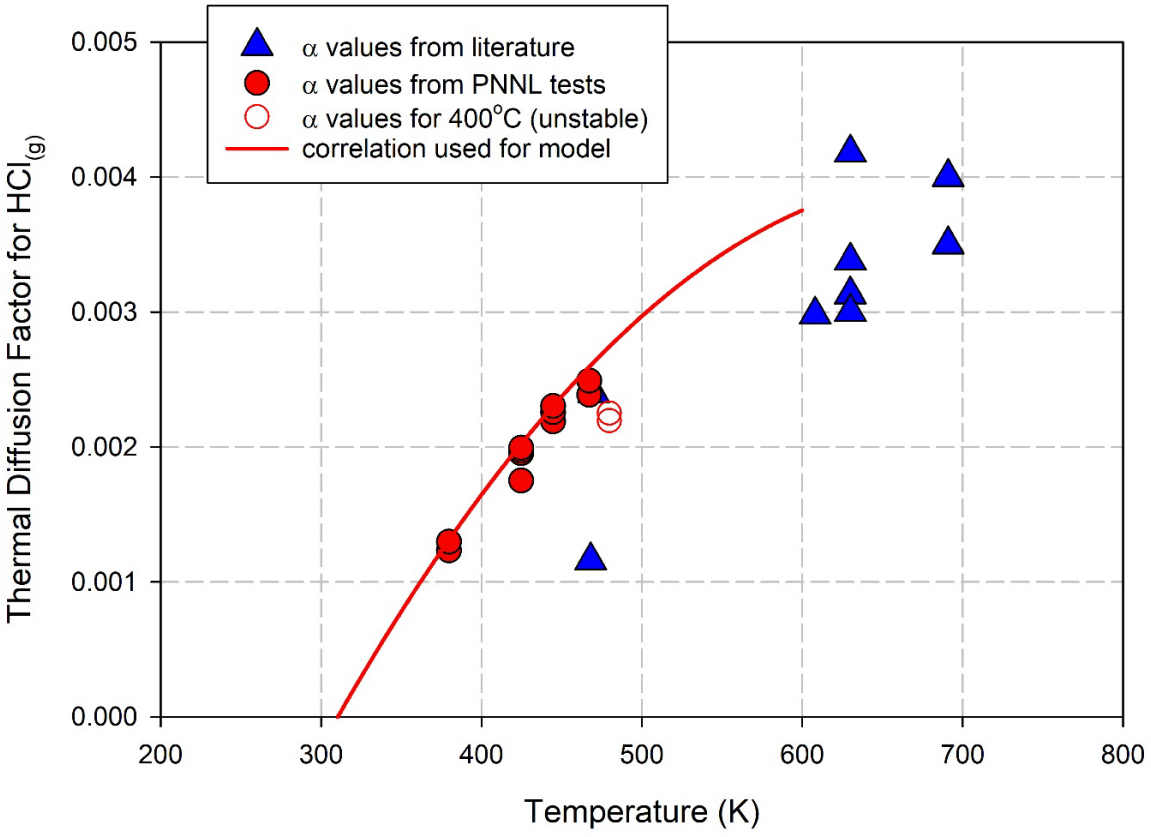

Figure 10: Comparison of PNNL and literature value measurements of the thermal diffusion constant, α, for $HCl_{(g)}$. The temperature plotted is the T_{avg} of the column. The red line is a correlation used for prediction during modeling efforts. The open red circles were not used in the correlation as the data was obtained under pressure and flow instability issues likely biasing the data low.

The pressure dependence of the thermal diffusion constant was also probed using the TDIS system. The pressure range of interest was chosen and bounded through early model predictions of ideal pressures based on the shape factors of the as-built system. Figure 11 shows the comparison of QQQ-ICP-MS measured ^{37}Cl mole fractions and the COMSOL MPP model predictions at the heavy end of the TDIS column as a function of varying $HCl_{(g)}$ pressure. The observed separation factors for each test were used to predict the heavy end concentration assuming the light end is fixed at natural abundance as would be the case during bleed and feed system operation. As can also be seen in Table 2, the data indicated little variation of α with pressures between 0.5 -1 atm. The model (curves) and measured fractions (data points) agreed except for one outlier at 290 °C and 0.63 atm. While this outlier is unexplained currently, the ideal pressures (highest α and therefore separation factor) are higher for this hot side temperature and obliviate the need for increased scrutiny at this time for the discrepancy between model and measured data.

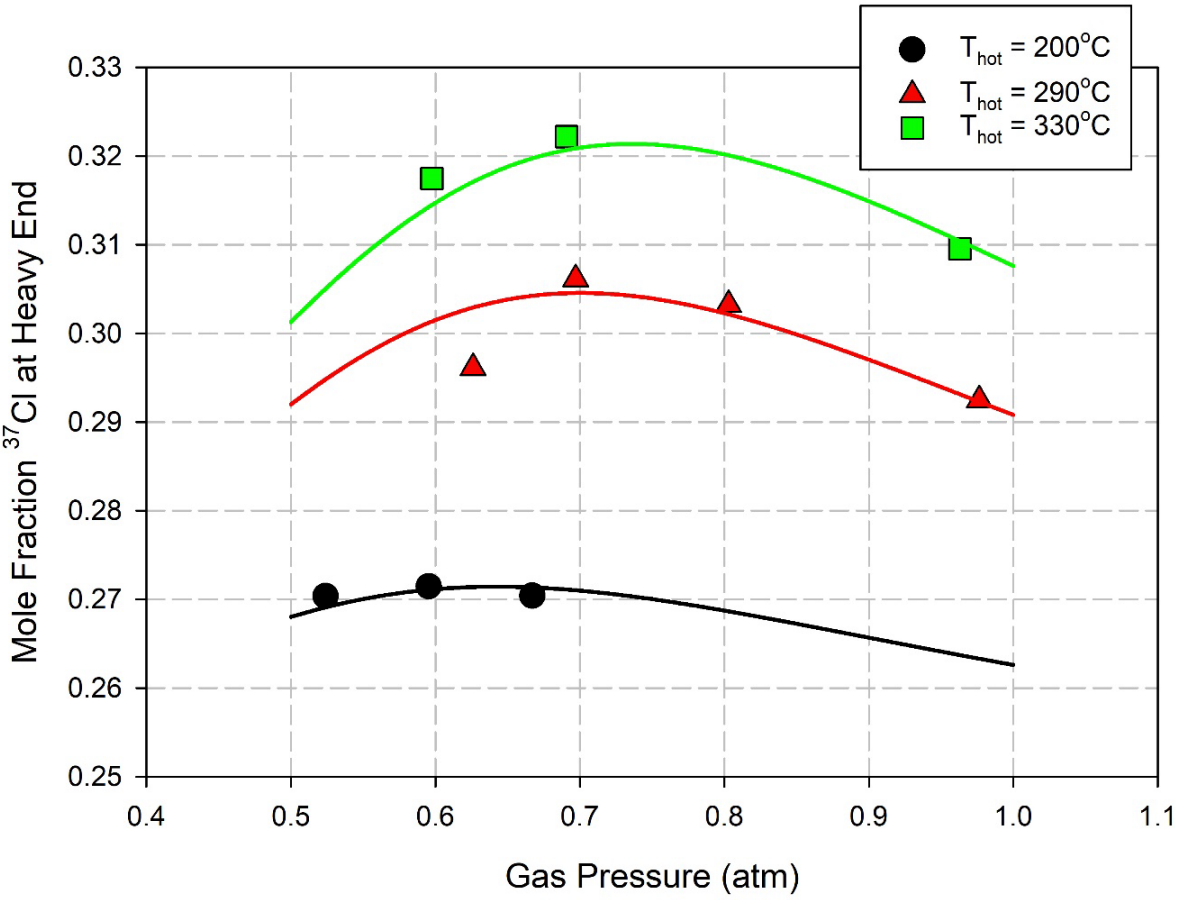

Figure 11: Measured and modeled pressure dependence of isotope separation for multiple temperatures.

4.3 Enrichment Predictions of Larger Scale TDIS Systems

Based on the data obtained and measured for the thermal diffusion coefficient and the pressure dependence of the as-built system, the validated COMSOL MPP model provides design predictions for larger scale TDIS systems. Figure 12 provides temperature dependent curves for needed column lengths to reach desired enrichment targets. These curves are based on the

measured data and extrapolations to higher temperatures based on the best fit line shown in Figure 10. This plot provides the design data needed for reaching higher enrichments than the small scale TDIS column used in the present work. As can be seen, 20 meters of total tube length with a hot side temperature of 500 °C will yield 98% ^{37}Cl under no flow (infinite reflux) conditions. It is important to note that this is under infinite reflux conditions. While under bleed and feed conditions, more length will likely be needed. For comparison, under the same length and no flow conditions, 400 °C will produce 92% enrichment, 300 °C produces 74%, and finally 200 °C produces 47% enrichment. While 200 - 300 °C produce significant drop off in enrichment per length of tubing, one can envision that 400 °C may be a good compromise of material durability and tube length. It is likely that temperatures above 400 °C (the max design temperature of this work) will produce significant corrosion. This temperature is likely approaching the limit of Inconel 600's use range with $HCl_{(g)}$ as was found in openly published literature data.

Preliminary disassembly of one column of Inconel 600 run at 400 °C showed no pitting corrosion, but it did exhibit a fine film of passivation that could be wiped off with a solvent. Considering the system's thermal expansion design limit of 400 °C, higher temperature testing was not conducted and in depth analysis of the corrosion/passivation layer formation was not undertaken during the present work.

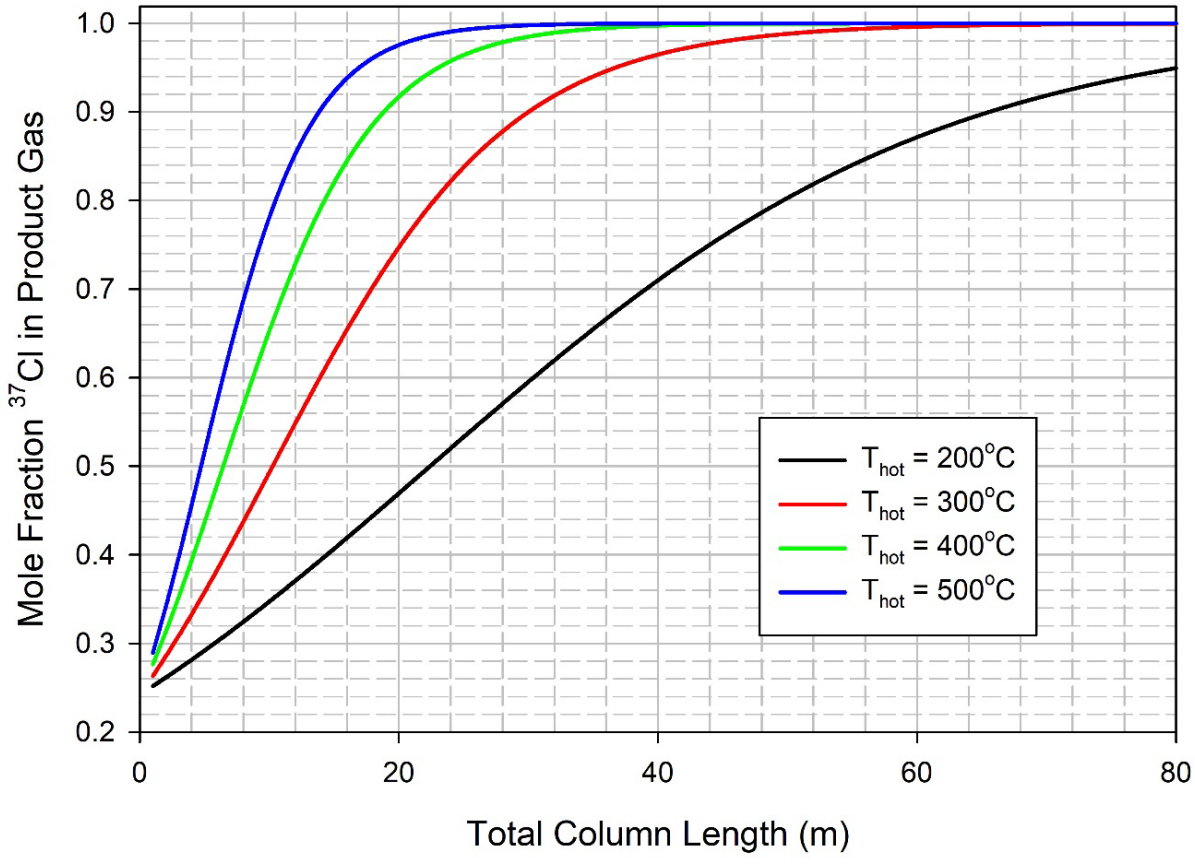

Figure 12: Enrichment levels that can be reached based on total TDIS column lengths for varying temperatures.

Regardless of materials of construction, a potential upper temperature limit for T_{hot} can be realized by consideration of the free energy of decomposition of HCl plotted as in Figure 13. HCl decomposition increases with temperature to produce hydrogen and chlorine gas (H_2 and Cl_2, respectively). If this occurred during the enrichment process, the chlorine would migrate with the heavy fraction and hydrogen with the light. The fact that the TDIS pioneers did not approach higher temperatures than shown in Figure 2 (and reproduced in Figure 10), indicates that they recognized the decomposition from their experimental results or that thermal heating greater than 700°C disturbed their system in some other manner. This is interesting because if the reason is not the former then improved materials of construction might allow access to higher enrichment capability. And even if the former is valid, then the proportion of Cl_2 formed might be separated by mass, down-stream of the HCl separation; a $H^{37}Cl/Cl_2$ separation.

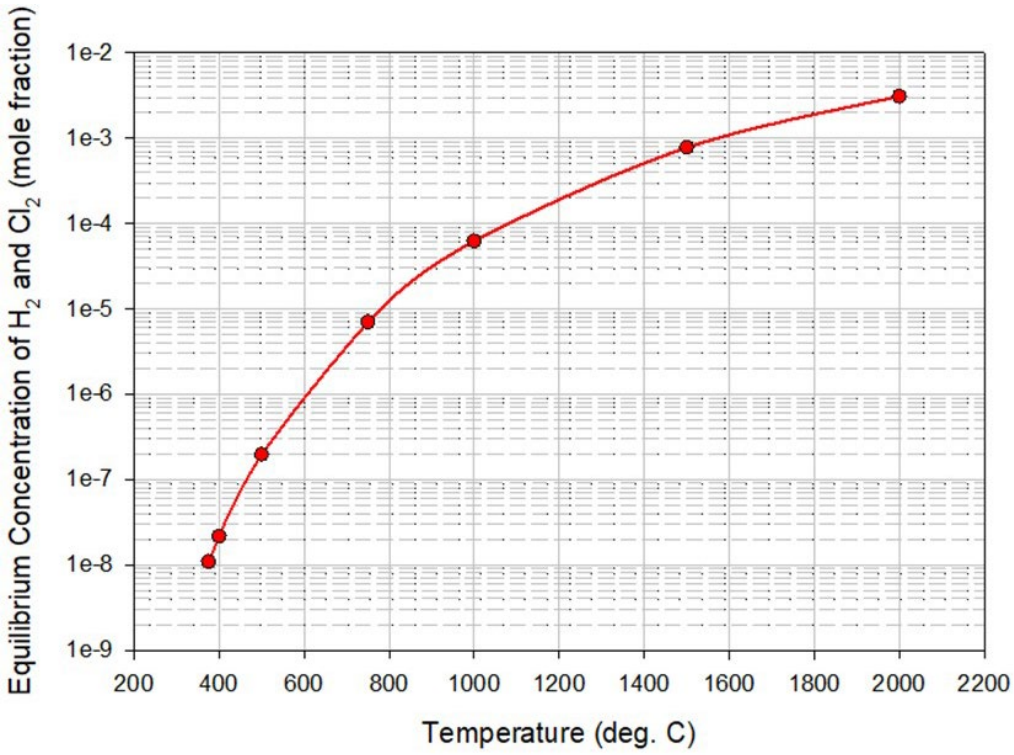

Figure 13: Calculated equilibrium concentrations of Cl_2 and H_2 gas from temperature dependent decomposition of HCl.

4.4 TDIS Facility Power Requirement Predictions

Early in the development of this project, the COMSOL MPP model was used to predict the cost of $H^{37}Cl$ product produced using bleed and feed operation for varying channel gap (between T_{cold} and T_{hot} walls), pressure, and column cost. This early work used the literature values of the thermal diffusion constant (Figure 2) and compared a long and short lifetime scenario where the tube cost differentiated the two scenarios. The short lifetime option considered relatively expensive columns ($6000 per meter) operated over a facility life of two years. The long lifetime option considered relatively inexpensive columns ($2000 per meter) operated over a twenty

year facility life. The power cost was kept constant at $0.15/kW-hr. The results of these analysis are shown in Figure 14 and Figure 15.

In the case of the long lifetime scenario, the power requirements of heating and cooling the columns are the major driver of cost. For all the channel gaps analyzed over varying operating pressures, the optimized product cost about $13 per gram of $H^{37}Cl$. Additionally, it is seen that smaller gaps allow for a larger operating window of optimum system pressure. In contrast, the short lifetime scenario, the cost driver is a combination of the system heating and cooling costs and the column manufacturing costs. In this scenario, the smaller channel gaps offer reduced costs because the total column length required is shorter for the smaller gaps.

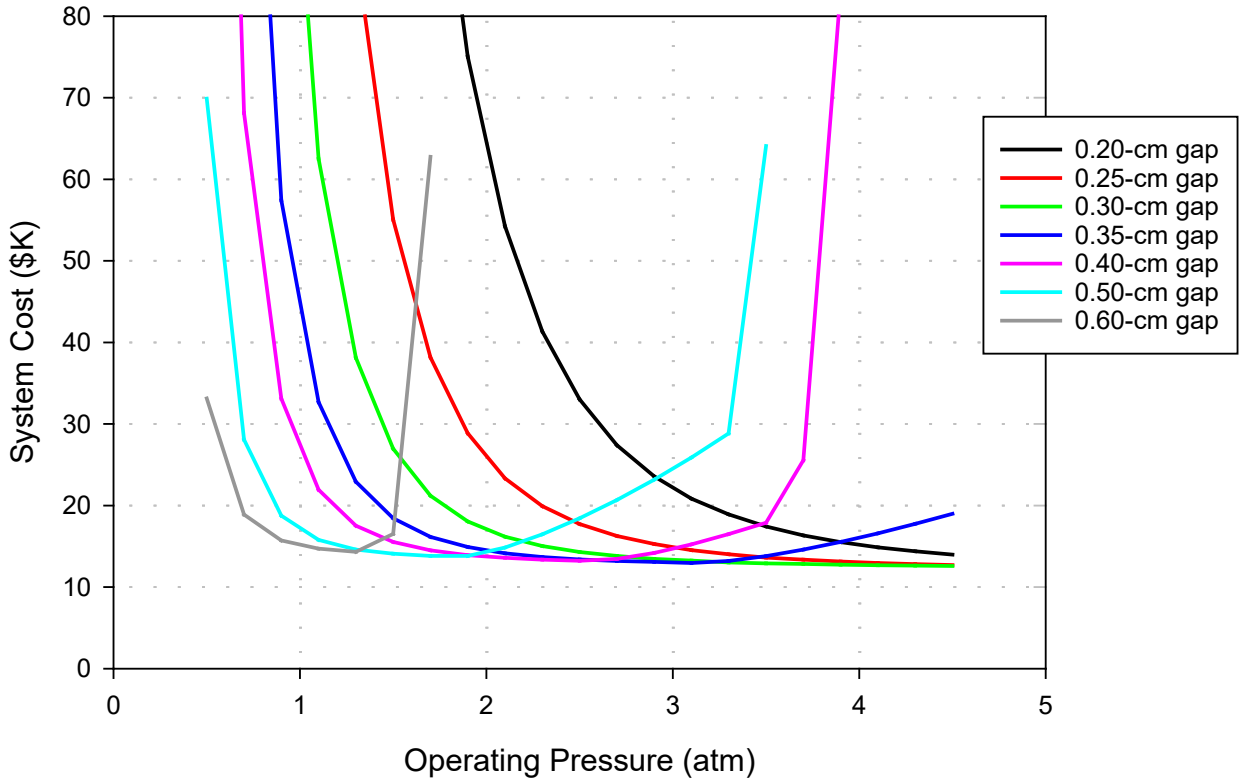

Figure 14: Long lifetime scenario where column costs are lower and the facility operates for a longer life.

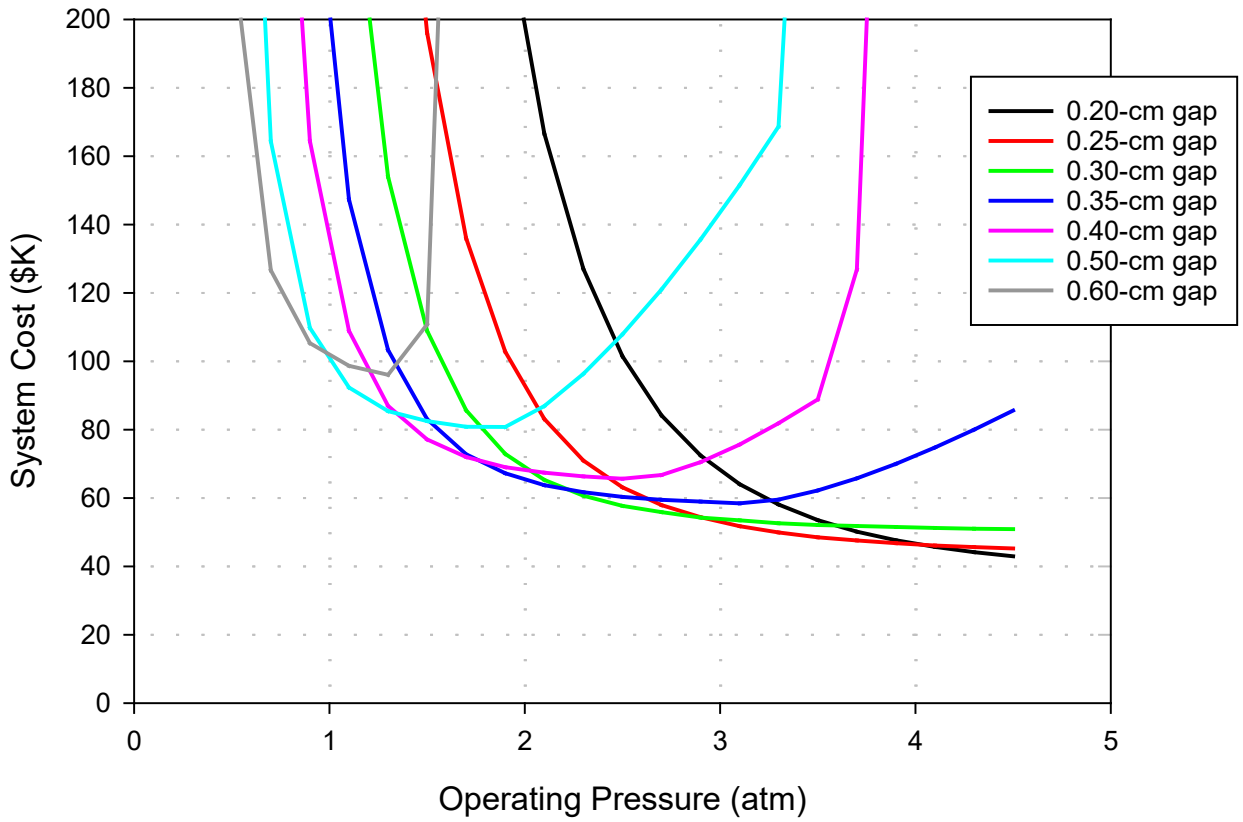

Figure 15: Short lifetime scenario where column costs are higher and the facility operates for a shorter length.

5.0 Future Work

In 2024, the project will aim to reach higher enrichments and produce an enriched $H^{37}Cl$ gas for use by the wider community. More tubes will be built and installed at PNNL and the validated model will be used to inform design. In addition to reaching higher enrichments, the project will work towards a tool that enables facility design. It is envisioned that a manufacturer would be able to provide operational and product criteria, and the team would be able to help in the design of a facility.

5.1 Serial and Cascade Tube Arrangements

Access to higher enrichments and rates of ^{37}Cl production using the metal columns developed at PNNL will initially come from a strategic numerical design of the number of columns and their serial or cascade arrangement. Examples for the number of serial columns required to reach successively higher enrichments in the heavy ^{37}Cl fraction are plotted in Figure 12. Additional factors beyond that of total column length and temperature also must be considered. Operational criteria will drive entry location of feed gas, the production rate, storage of gas in cylinders, and the needed enrichment. The validated TDIS model in COMSOL MPP will greatly increase the ability to predict and design the serially aligned tubing cascades envisioned for meeting a product demand.

5.2 Materials of Construction

We have discussed that the early measurements of the thermal diffusion constant, α, as shown in Figure 2 by (Akabori 1941, Clusius 1939, Kennedy 1940, Kranz 1953, Shrader 1946) were acquired between 600-700°C. The separations were done in fact at temperatures exceeding 600°C and were made possible by the use of glass separations columns. The use of glass as the material of construction at 7 meter lengths, then and today, represents a safety hazard. We can imagine multiplication of perhaps thousands of these tubes for the production operation. Glass tubes could be encapsulated in metal housings to increase the safety aspect of the operation. Several other issues are recognized, again not for a single tube but rather its extension to multiple tubes. The tube within a tube design we have developed (Figure 1) requires that a highly accurate gap tolerance is maintained through the length of the separations device and a cooling jacket needs to be present on the outer wall for maintenance of T_{cold}. One can envision then a very large condenser. The connections to successive stages might be glass or metal and would require appropriate glass to metal seals. Kovar® provides a common glass to nickel metal seal, albeit a delicate one. Other connective glass to metal seals for gas inlets and gas sampling are required. The construction of a safe, glass apparatus for multiple separations stages is a research project on its own. The time for development and construction of a serial arrangement of the devices appears not defensible.

Something prevented the pioneers from taking their enrichment to higher temperatures. It may have been that the HCl decomposition became intolerable (Figure 13), or simply the power to heat their central heater (T_{hot}) to a stable value in the 7 meter tube was not possible at their facility. Another possibility is that contaminants in the glass were solubilized from the glass in the hot HCl and caused problems. Regardless, this is a new space to investigate. Potentially 700 - 800°C separations with some production of hydrogen gas and chlorine gas could be managed. But this requires materials of construction that are compatible with that temperature and a highly corrosive working gas.

Another area of outward reach for materials of construction that might be compatible with hot HCl gas are silicon/silica, gold, or platinum coatings on metals or intermetallics. First, we have not established a vendor in the United States for any of these that also has the capability to provide long metal tubes. Generally, the tubes are cut to approximately six meter lengths. It is possible that if appropriate coatings of these tube exteriors could be made, the coupling of preferably three tubes (height minus required losses due to fabrication) would be possible with special engineering at each coupler. But the problem doesn't stop there; thermal mismatch of a coating on the metal is integral to the high temperature stability of the coating.

Research on metal coatings of various processed silicas is a long-standing and some new technologies show promise (Silcotek 2023). For our case (Figure 1), the use of metal ball bearings, that hold the gap integrity, might crush silica-based coatings, whereas the use of glass ones might accommodate the thermal stresses the apparatus undergoes on heating to operational temperatures. Gold coatings on the best metal surfaces, surprisingly are not yet stable to high temperatures. Intermetallics, ceramics (Allendorf 1993), and refractory metal oxides and fluorides may be the best hope in the near future, and several are already used for high temperature applications, e.g., heating elements, turbine engines, etc. Having solved the thermal mismatch problem, it would seem the platinum aluminides may show promise. Preparative applications of the later grouping of coating types are well understood on nickel-based metals for instance and could be used for the larger scale tubes required here [Yuan 2013]. Most have not been tested under the conditions of the TDIS apparatus. The time for research and development of these products is again not defensible for the Chlorine Isotopes Team at PNNL to pursue at this time, with respect to budget and anticipated demand. The technologies are under active research especially with the expected arrival of MSR that use chloride and fluoride salts at high temperature.

6.0 Conclusions

Beginning in 2023, a separations apparatus for enrichment of the ^{37}Cl in natural isotopic composition of HCl was initiated by the Chlorine Isotopes Team at PNNL. Data from the literature was used for an initial set of estimates that culminated in the design and construction of the first separations device. The device was relatively short and made of metal. Both deficiencies were anticipated from work done historically. The geometric construction of the device was guided by numerical simulation. Early data acquisition proved that the simulations worked well in several aspects of construction and then in its operation. The model that was established is predictive of the separations column efficacy, thus is now a useful tool for design of larger separation systems. The prognostic capability of the model allows us now to numerically increase separations efficiency and to understand how rates of the ^{37}Cl will be optimized. Valuable data points for the coefficient of thermal diffusion were found with high precision helping to fill in gaps from the existing historical data set.

There is no doubt that better materials of construction will more promptly allow enrichment and production. We know this also from the model. However, for these initial current studies, their costs are prohibitive, and the Team has decided to push forward with extension of the existing system to explore rates of production, that may use serial production, re-enrichment, and distributed cascading schemes. The Chlorine Isotopes Project Team at PNNL is prepared to claim that the installation and hence its separative power is restricted only by the spatial limitations of the laboratory, and this at present appears to be the limiting feature to first pass high enriched ^{37}Cl.

7.0 References

- Abramychev, S .M., N.V. Balashov, S.P. Vesnovskii, V.N. Vjachin, V.G. Lapin, E.A. Nikitin, V.N . Polynov. “Electromagnetic separation of actinide isotopes.” *Nuclear Instruments and Methods in Physics Research* B70 (1992): 5-8

- Akabori, K., S. Husimi, S. Kikuchi, M. Kohayashi, Y. Ko; T Momota, H.Nagaoka, M. Okazaki, I. Suehiro, E. Takeda, M. Taketani, T. Utiyama,T. Wakatuki, Y. Watase, S. Yamaguchi, I. Yukawa. “Separation of Isotopes by Thermal Diffusion, II. Separation of Chlorine Isotopes, *Osaka Nuclear Physics Laboratory* 23 (1941): 500-604.

- Allendorf, M D, Outka, D A. “The reactivity of HCl and methyltrichlorosilane with silicon carbide surfaces.” *Materials Research Society (MRS) symposiu*m, Boston, MA, 1993

- Borisevich, V. D., O. E. Morozov, Yu. P. Zaozerskiy, G. M. Shmelev, Y. D. Shipilov. “On the enrichment of low-abundant isotopes of light chemical elements by gas centrifuges.” *Nuclear Instruments and Methods in Physics Research A*, (2000): 515-521

- Bouchez, C., Pupier, J., Benedetti, L., Deschamps, P., Guillou, V., Keddadouche, K., Aumaître, G., Arnold, and M., Bourles, D. Isotope Dilution-AMS technique for 36Cl and Cl determination in low chlorine content waters. *Chemical Geology* 404 (2015): 62-70.

- Chapman, Sydney, and F. W. Dootson. "XXII. A note on thermal diffusion." *The London, Edinburgh, and Dublin Philosophical Magazine and Journal of Science* 33, no. 195 (1917): 248-253.

- Clusius and Dickel, “Das Trennrohr. II. Trennung der Chlorisotope.” Zeitschrift fur Physikalische Chemie. 44B (1939): 451-473 (in German)

- Enskog, D. "Remarks on a fundamental equation in kinetic gas law." *Physik. Zeits*, 12 (1911): 533

- Enskog, D., “Kinetische Theorie der Vorgänge in Mässig Verdünnten Gasen.” Doctoral Dissertation, Uppsala, 1917

- Fujitani, T., and Nakamura, N. “Determination of Chlorine in Nine Rock Reference Materials by Isotope Dilution Mass Spectrometry.” *Geostandards and Geoanalytical Research* 30 (2006): 113-120.

- de Gois, J.S., Costas-Rodriguez, M., Vallelonga, P., Borges, D.L.G., and Vanhaecke, F. “A simple method for high-precision isotope analysis of chlorine via pneumatic nebulization multi-collector inductively coupled plasma-mass spectrometry.” *Journal of Analytical Atomic Spectrometry* 31 (2016): 537-542.

- Greene, Hoglund, and Von Halle. “Thermal Diffusion Column Shape Factors: Part I. Shape Factors Based on an Inverse Power Repulsion Model. Report No. K1469. Union Carbide Corp., Oak Ridge, TN, 1966

- Harkins, W. D., A. Hayes. “The separation of the element chlorine into isotopes” Vol. XIX., No. 4. *Phys. Rev.19* (1922): 403-404

- Kaliteevskny, A. K., O. N. Godisov, V. P. Liseikin, B. V.Tyutin, L. P. Myazin, L. Y. Safroiov, A. I. Glazunov. “Development of the design of a new generation gas centrifuge for separation of stable isotopes” (2023) https://inis.iaea.org/collection/NCLCollectionStore/_Public/34/083/34083415.pdf?r=1

- Kemp, R.S. “Gas centrifuge theory and development: a review of US programs.” *Science and Global Security 17* (2009): 1-19.

- Kennedy and Seaborg. “Isotopic Identification of Induced Radioactivity by Bombardment of Separated Isotopes; 37-Minute Cl^{38}.” *Phys. Rev.* 57 (1940): 843-844.

- Kondev, F. G., Meng Wang, W. J. Huang, S. Naimi, and G. Audi. "The NUBASE2020 evaluation of nuclear physics properties." *Chinese Physics C* 45, no. 3 (2021): 030001.

- Kranz and Watson. “Chlorine Isotope Separation by Thermal Diffusion.” *Phys. Rev.* 91(6) (1953): 1469-1472.

- Lindauer, R. B. MSRE design and operations report: Part VII, Fuel handling and processing plant, ORNL TM-907, 1967

- McNamara, B. K., Z. F. Huber, M. R. Powell, T. Schlieder, J. M. Davis, T. G., Levitskaia, J. S. Cervantes, C. A. Lowrey, N. D. Rocco, M. L. Di Vacri, I. Arnquist, D. Clelland, 0BChlorine Isotope Separations using Thermal Diffusion, PNNL-34297, Pacific Northwest National Laboratory, 2023

- Ohata, M., Zhu, Y., and Nonose, N. “Studies on Isotope Ratio Measurement of Cl by Inductively Coupled Plasma Triple-quad Mass Spectrometry.” *Analytical Sciences* 33 (2017): 375-380.

- Rae, H. K. “Selecting Heavy Water Processes.” *American Chemical Society* (1978): 1–26

- Renpenning, J., Hitzfeld, K.L., Gilevska, T., Nijenhuis, I., Gehre, M., and Richnow, H.-H. “Development and Validation of an Universal Interface for Compound-Specific Stable Isotope Analysis of Chlorine (37Cl/35Cl) by GC-High-Temperature Conversion (HTC)-MS/IRMS.” *Analytical Chemistry* 87 (2015): 2832-2839.

- Rutherford, E., Soddy, F. “Radioactive Change” *The London, Edinburgh and Dublin Philosophical Magazine and Journal of Science* 5:29 (1903): 576-591,

- Shrader, E.F. “Partial Separation of the Isotopes of Chlorine by Thermal Diffusion.” *Phys. Rev.* 69 (1946): 439-442

- Silcotek, https://www.silcotek.com/blog/silcolloy-2000-a-new-cvd-coating-for-high-temperature-stability-and-corrosion-resistance. 2023

- Smith, M. L. “Electromagnetic enrichment of stable isotopes.” *Progress in Nuclear Physics*, Volume 6, (2013): 162-191

- Soddy, F. "The Origins of the Conception of Isotopes-Nobel Lecture." *December* 12 (1922) https://www.nobelprize.org/prizes/chemistry/1921/soddy/lecture/

- Thompson, J. J. “Rays of Positive Electricity*” Proceedings of the Royal Society*, Section A, Mathematical and Physical Sciences (1913): 1-20

- Vengosh, A., Chivas A.R., McCulloch M.T.. "Direct determination of boron and chlorine isotopic compositions in geological materials by negative thermal-ionization mass spectrometry." *Chemical Geology: Isotope Geoscience Section* 79.4 (1989): 333-343.

- Vogel, D. J., Nenoff, T.M., Rimsza J.M. “Design Elements for Enhanced Hydrogen Isotope Separations in Barely Porous Organic Cages” *ACS Omega*. 7(9) (2022): 7963–7972, doi: 10.1021/acsomega.1c07041

- Xiao, Y. K., Yinming, Z., Quingzhong, W., Haizhen, W., Weiguo, L., and Eastoe, C.J. “A secondary Isotopic reference material of chlorine from selected seawater.” *Chemical Geology* 182 (2002): 655-661

- Yuan, K. “Thermal and Mechanical Behaviors of High Temperature Coatings” Linköping University, 581 83, Linköping, Sweden, Linköping Studies in Science and Technology, Thesis No. 1569 (2013)

Appendix A – Key Team Members and Co-Investigators

Bruce McNamara (PI):
Bruce McNamara is a Chemist in the Actinide Chemistry Team at PNNL. He is the Principal Investigator for this project and works on system design and operations. He holds a PhD in physical chemistry from Purdue University. Bruce brings decades of experience in analytical gaseous chemistry and is an established expert in fluorination of actinides. Bruce currently works on national security missions for fluorination of uranium and conversion/deconversion using gaseous chemistry as well as many nuclear energy projects relating to fluorination.

Zach Huber (PM):
Zach Huber is a Mechanical Engineer at PNNL in the Nuclear Process Engineering Team at PNNL. He is the Project Manager for this project and works on system design and operations. He received his M.S. and B.S. in mechanical engineering from University of Texas - San Antonio. He is currently the NA231/USHPRR silicide fuel fabrication manager for converting the high flux isotope reactor to HALEU fuel from the current HEU oxide fuel. He also works on multiple other uranium research projects ranging from fabrication to fluorination.

Mike Powell:
Mike Powell is a chemical engineer and leader of the Process Intensification Team at PNNL. He leads the work on system design, operation, and multi-physics modeling. His research interests include compact chemical reactors, heat exchangers, and advanced separation technologies. He received a MS in chemical engineering from Washington State University and joined PNNL in 1990.

Tatiana Levitskaia:
Tatiana Levitskaia is a Chemist and leader of Radiochemical Science Team. She works on system operations. Tatiana received her PhD in chemistry from Brigham Young University. She has over 25 years of R&D experience, a strong record of scientific innovation and generation of creative solutions to challenging fundamental and applied problems in the area of separation sciences. She has extensive experience in design and validation of separation processes for the nuclear fuel cycle.

Juan Cervantes
Juan Cervantes is a Post-Bachelor Research Associate in the Radiochemical Science Team at PNNL. He is helping with key tasks on this project including procurements and system operation. He received a B.S. in chemistry from the University of Washington. Juan currently works on various projects under the direction of his mentor, Tatiana Levitskaia. Other projects he is currently working on include the alkaline dissolution of uranium, iodine separations in the PUREX flowsheet, and the recovery of rare earth metals from phosphate sludge waste.

Parker Okabe
Parker Okabe is a Materials Scientist in the Actinide Processing Group at PNNL. He is helping develop a method for analyzing the chlorine isotope ratio HCl-38/HCl-36 in real-time using a residual gas analyzer. He received a B.S. in Mechanical Engineering and a Ph.D. in Nuclear Engineering at the University of Utah. Parker currently works on various projects under the direction of his mentor, Richard Clark. Other projects he is currently working on include various system instrumentations and controls, pyroprocessing of uranium and plutonium, and CAD design.

Riane Stene
Riane Stene is a Material Scientist in the Engineered Materials group at PNNL. She supports this project and works on system design, operations, and experiment execution. She holds a Dr. rer nat (German Ph.D. equivalent) in Physics from the Technical University of Munich. Riane is well versed in fluorine chemistry and fluoride separation, having over 7 years of experience in the field. Riane supports a variety of projects at PNNL, including projects related to national security, nuclear safeguards, and quantum computing.

Tyler Schlieder:

Tyler Schlieder is a chemistry Post-Doctoral Research Associate in the Ultra-Low Background Materials Team at PNNL. For this project he works on measuring Cl isotopic ratios via triple quadrupole (QQQ)-ICP-MS to validate ^{37}Cl enrichment efforts. He received his B.S. from Oregon State University, M.S. from Northern Arizona University, and Ph.D. from UC Davis, all in Geology/Geochemistry. Tyler currently works primarily supporting rare-event physics experiments. He also is involved in characterizing different mass spectrometry methods for use in making ultra-sensitive nuclear measurements

Appendix B – Conferences and Publications

- T. D. Schlieder N. D. Rocco, M. di Vacri, I. J. Arnquist, D.R. Bottenus, Z. F. Huber, B. K. McNamara. 01/20/2024. Rapid determination of chlorine isotopic ratios using qqq-icp-ms/ms with o_2 gas: application to molten salt reactor (msr) research. Presented by T. D. Schlieder at Winter Conference on Plasma Spectrochemistry, Tucson, Arizona. PNNL-SA-193910.

- B. K. McNamara, Z. F. Huber, M. R. Powell, T. G. Levitskaia, T. D. Schlieder, Chemistry of fuel cycles for molten salt reactor technologies. Presented by B. K. McNamara at the International Atomic Energy Agency, IAEA, Vienna, 2-6 October 2023.

- B. K. McNamara, Z. F. Huber, M. R. Powell, T. G. Levitskaia, T. D. Schlieder, Chlorine isotopes separation for fast spectrum msr, Presented by B. K. McNamara at the Annual MSR Campaign Review Meeting 2-4 May 2023.

- T.D. Schlieder, N.D. Rocco, M. di Vacri, I.J. Arnquist, D.R. Bottenus, B.K. McNamara, Z.F. Huber. “Rapid and accurate determination of Cl isotope ratios in diverse sample matrices with QQQ-ICP-MS/MS using an O_2 reaction gas.” *(Manuscript in preparation)*

Appendix C – Chlorine Isotopes Measurement and Validation

(Reproduced from McNamara 2023)

We have developed a method for measuring chlorine isotopic ratios using triple-quadrupole inductively coupled plasma mass spectrometry (QQQ-ICP-MS) as a means of validating ^{37}Cl enrichment. Chlorine isotopic ratios can be measured using a number of analytical techniques including thermal ionization mass spectrometry (Vengosh 1989, Fujitani 2006), accelerator mass spectrometry (Bouchez 2015), and isotope ratio mass spectrometry (Renpenning 2015). While these techniques are capable of accurate and precise chlorine isotopic ratio measurements, they require complicated and time-consuming front-end chemistry/analyses and/or costly instrumentation.

More recently, ICP-MS techniques have received increased attention for making Cl isotopic ratio measurements. Advantages of ICP-MS over other analytical techniques include reduced need for complicated instrumentation and more rapid sample throughput. However, accurate and precise determination of Cl isotopic ratios by ICP-MS is hindered by spectral interferences caused by polyatomic ions, primarily $^{16}O^{18}O^{1}H$ and $^{36}Ar^{1}H$, which interfere with ^{35}Cl and ^{37}Cl, respectively. One way to overcome this hindrance is with the use of the high mass resolving power of a multi-collector ICP-MS (de Gois 2016, Ohata 2017). While this approach has been demonstrated to be effective (de Gois et al., 2016), it still requires costly instrumentation and significant sample preparation to isolate the target analyte from the sample matrix (de Gois 2016). An alternative means of eliminating problematic polyatomic interferences is using a QQQ-ICP-MS in combination with a reaction gas such as O_2 (Ohata et al., 2017). We take this approach.

All Cl isotopic ratios were measured using an Agilent 8900 QQQ-ICP-MS (Agilent Technologies Inc., Santa Clara, CA, USA). This instrument consists of two quadrupole mass filters and an octupole collision/reaction cell (ORC). The ORC is set between the two mass filters, referred to herein as Q1 and Q2. For these types of analyses the instrument is operated in MS/MS mode, where each mass filter act as an ion guide and can pass any selected mass *m/z* with unit mass resolution. In this case, Q1 is set to allow *m/z* = 35 and 37 to pass into the ORC. Once in the ORC, Cl reacts with O_2 to produce $^{35}Cl^{16}O$ and $^{37}Cl^{16}O$, effectively separating Cl from potential polyatomic interferences at *m/z* = 35 and 37. The second mass filter, Q2, is then set to *m/z* = 51 and 53, allowing the mass-shifted Cl isotopes to pass into the detector. The Cl isotopic ratio is then determined as 53/51, which corresponds to $^{37}Cl^{16}O/^{35}Cl^{16}O$.

We initially validated this method by measuring the Cl isotopic ratio in hydrochloric acid (HCl) and comparing our results to the natural Cl isotopic ratio (0.31977; Xiao 2002) represented by standard mean ocean chlorine. Our measured Cl isotopic ratio ($^{37}Cl/^{35}Cl$ = 0.3165 ± 0.0015, *n=5*) differed from the natural ratio by 1.01%. We also validated this method by measuring Cl isotopic standard NIST SRM 975a ($^{37}Cl/^{35}Cl$ = 0.31970 ± 0.00006). The NIST standard was NaCl dissolved in water. We report a chlorine isotopic ratio for NIST SRM 975a of $^{37}Cl/^{35}Cl$ = 0.3195 ± 0.0008 (*n=3*) which deviates from the certified value by <0.1% (Fig. 7). These data indicate our method can measure natural Cl isotopic ratios with an accuracy of <1%. In order to validate this method for enriched Cl isotopic ratios, we measured solutions that had been spiked with a known amount of enriched Cl reference material (ERM®-AE642, $^{37}Cl/^{35}Cl$ = 55.24). We then constructed Cl isotopic ratio calibration curves. We performed this exercise with a simple HCl matrix ($^{37}Cl/^{35}Cl$ = 0.3197 - 1.8791). Resulting calculated and measured Cl isotopic ratios are in good agreement (R^2 = 0.9999; Fig. 8), indicating we can accurately determine enriched Cl isotopic ratios at least up to $^{37}Cl/^{35}Cl$ =1.8971.

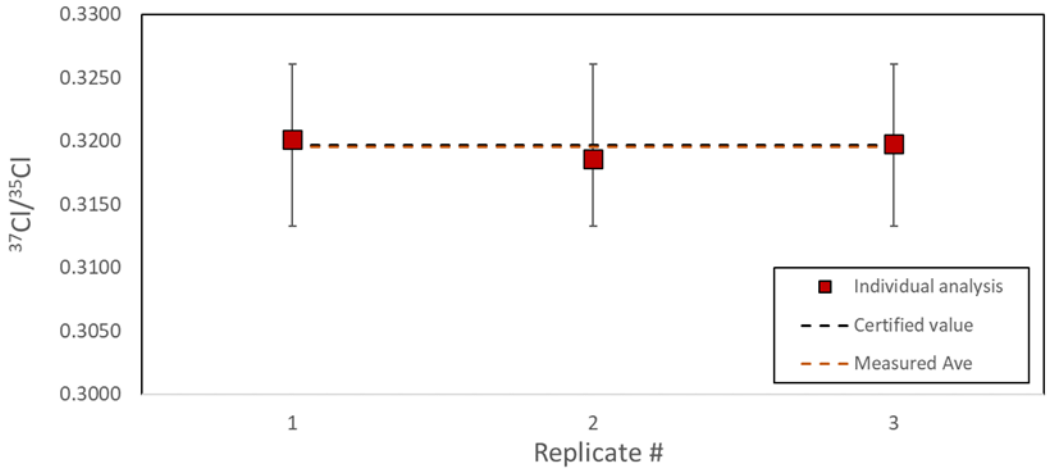

Figure C1: Replicate analysis of Cl isotopic standard NIST SRM975a using our QQQ-ICP-MS method.

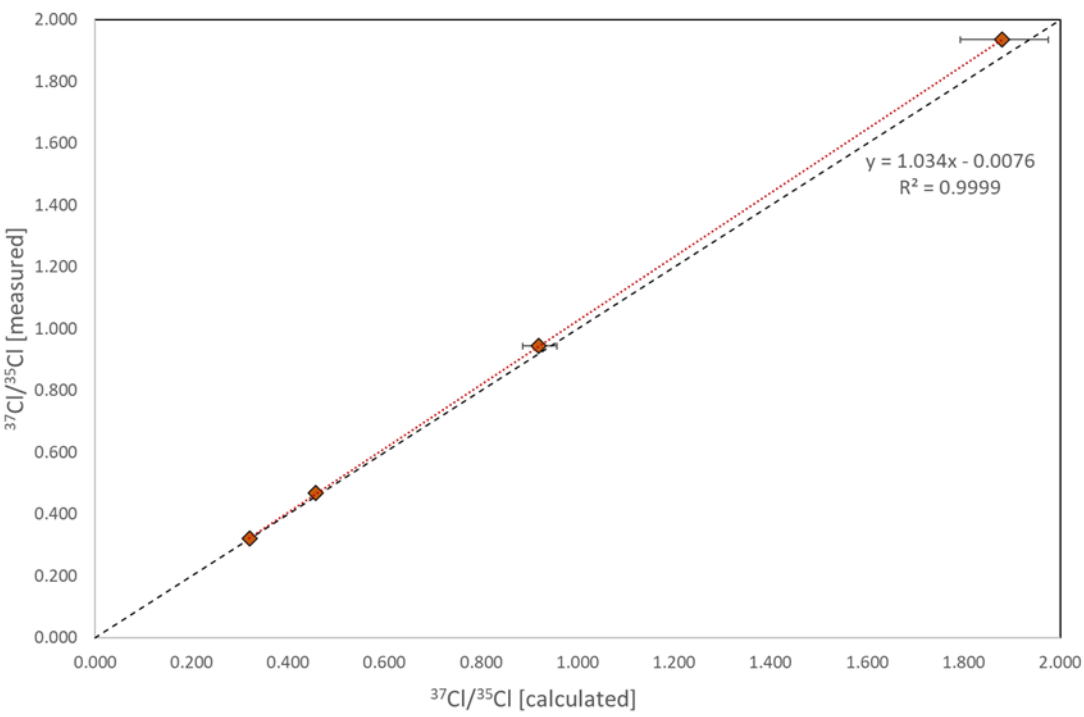

Figure C2: Calibration curve for variable Cl isotope ratios within an HCl matrix.

Pacific Northwest National Laboratory

902 Battelle Boulevard
P.O. Box 999
Richland, WA 99354

1-888-375-PNNL (7665)

www.pnnl.gov